EJNMMI RESEARCH

ORIGINAL RESEARCH

Open Access

The added values of ^{18}F-FDG PET/CT in differentiating cancer recurrence and osteoradionecrosis of mandible in patients with treated oral squamous cell carcinoma

Nai-Ming Cheng[1,2], Chien-Yu Lin[3], Chun-Ta Liao[4], Din-Li Tsan[3,5], Shu-Hang Ng[6] and Tzu-Chen Yen[1*]

Abstract

Background Osteoradionecrosis (ORN) of the jaw requires a differential diagnosis to exclude cancer recurrence. Here, we sought to develop a scoring system comprising ^{18}F-FDG PET/CT parameters for distinguishing between the two conditions in patients with oral squamous cell carcinoma (OSCC).

Methods The study consisted of 103 OSCC patients with suspected ORN of the jaw. All participants underwent ^{18}F-FDG PET/CT imaging within 6 months of diagnostic histopathology. Following extraction of PET parameters, we identified clinical and imaging predictors of mandibular recurrence-free survival (MRFS) using receiver operating characteristic curve analysis and multivariate Cox regression models.

Results The results of histopathology revealed mandibular cancer recurrence in 24 patients (23.3%). Multivariate Cox regression analyses identified an age at diagnosis $\leq$ 52 years ($P = 0.013$), a location of the SUVmax voxel with soft tissue predominance ($P = 0.019$), and mandibular total lesion glycolysis (TLG) > 62.68 g ($P < 0.001$) as independent risk factors for MRFS. A scoring system was devised with scores from 0 (no risk factor) to 3 (presence of all three risk factors). High-risk patients with a score of 2–3 compared with score of 0–1 had a significantly higher likelihood of mandibular cancer recurrence (hazard ratio: 32.50, 95% confidence interval: 8.51–124.18, $P < 0.001$). The scoring system had a sensitivity of 87.50%, a specificity of 82.28%, and an accuracy of 83.50% for identifying mandibular cancer recurrence.

Conclusions The scoring system of our study is clinically useful for identifying mandibular cancer recurrence in patients with suspected ORN of the jaw.

Keywords PET/CT, Total lesion glycolysis, Oral cancer, Osteoradionecrosis, Recurrence

*Correspondence:
Tzu-Chen Yen
yentc1110@gmail.com
[1]Department of Nuclear Medicine and Molecular Imaging Center, Chang Gung Memorial Hospital, Linkou, Chang Gung University College of Medicine, No. 5, Fu-Shin St., Kueishan District, Taoyuan City 333, Taiwan
[2]Department of Nuclear Medicine, Chang Gung Memorial Hospital, Keelung, Keelung, Taiwan
[3]Department of Radiation Oncology, Chang Gung Memorial Hospital, Linkou, Chang Gung University College of Medicine, Taoyuan, Taiwan
[4]Department of Otolaryngology – Head and Neck Surgery, Chang Gung Memorial Hospital, Linkou, Chang Gung University College of Medicine, Taoyuan, Taiwan
[5]Department of Radiation Oncology, Chang Gung Memorial Hospital, Keelung, Taiwan
[6]Department of Diagnostic Radiology, Chang Gung Memorial Hospital, Linkou, Chang Gung University College of Medicine, Taoyuan, Taiwan

Springer Open

© The Author(s) 2023. **Open Access** This article is licensed under a Creative Commons Attribution 4.0 International License, which permits use, sharing, adaptation, distribution and reproduction in any medium or format, as long as you give appropriate credit to the original author(s) and the source, provide a link to the Creative Commons licence, and indicate if changes were made. The images or other third party material in this article are included in the article's Creative Commons licence, unless indicated otherwise in a credit line to the material. If material is not included in the article's Creative Commons licence and your intended use is not permitted by statutory regulation or exceeds the permitted use, you will need to obtain permission directly from the copyright holder. To view a copy of this licence, visit http://creativecommons.org/licenses/by/4.0/.

Introduction

While being an integral part of the multidisciplinary management of oral squamous cell carcinoma (OSCC), radiotherapy (RT) might cause various complications—of which mandibular osteoradionecrosis (ORN) is one of the most feared. Published data suggest that the prevalence of this condition following RT varies from 2 to 9%, with the main risk factors being age > 55 years [1, 2], active smoker at diagnosis [3] and RT doses > 60 Gy [4]. In general, ORN can be defined as an area of exposed devitalized irradiated bone that fails to heal over a period of three months without signs of recurrent or residual malignancy [5, 6]. The pathogenesis of ORN is complex and includes local inflammation, damage to vascular supply as a result of surgery or obliterative endarteritis, and altered bone healing accompanied by an increased susceptibility to infections [7–9].

Due to distinct clinical management, mandibular ORN requires a differential diagnosis to exclude tumor recurrence. Although ^{18}F-FDG PET/CT imaging is widely used in the evaluation of therapeutic outcomes and post-treatment surveillance of patients with OSCC [10], there are limited data on its potential usefulness for distinguishing between mandibular ORN and cancer recurrence. On analyzing a sample of 37 patients with head and neck malignancies arising from different anatomical sites, Meerwein and coworkers [11] have previously shown that a combination of three parameters—i.e., a low maximum standardized uptake value (SUVmax), the location of SUVmax voxel within the bone, and the presence of a pathological fracture—was independently associated with ORN. However, there was a significant overlap of SUVmax measurements between recurrent cancer and ORN [12, 13]—a finding attributable to the increased FDG uptake elicited by both hypoxia and bone tissue inflammation [14, 15]. In recent years, there has been significant interest in extracting quantitative information from PET images, i.e., radiomics, to improve the prediction accuracy of clinical outcomes [16–18]. In this scenario, we designed the current retrospective study to examine whether ^{18}F-FDG PET/CT functional parameters may be clinical useful for distinguishing between mandibular ORN and cancer recurrence in patients with OSCC.

Patients and methods

Study participants

The present retrospective study was conducted using reviewing chart records from patients with OSCC who had been diagnosed between April 2004 and April 2021 in the Chang Gung Memorial Hospital (Linkou, Taiwan). All participants had undergone primary treatment with curative intent—including RT with a total delivered dose > 50 Gy—and had suspected mandibular ORN clinically by chart records. Patients underwent ^{18}F-FDG PET/CT imaging and histopathological work-up for the diagnosis of mandibular lesions within the subsequent six months. Patients who achieved complete remission from a previous malignancy for at least 1 year were eligible for inclusion. Subjects with persisted second primary malignancies or aged less than 20 years were excluded, as were those with evidence of metastatic disease at presentation. The study protocol was approved by the Institutional Review Board of Chang Gung Medical Foundation (approval numbers: 202102071B0). The requirement for written patient informed consent was waived due to the study design. Our study was performed in accordance with the ethical standards as laid down in the 1964 Declaration of Helsinki and its later amendments or comparable ethical standards.

Post-treatment surveillance, staging, and data collection

According to our institutional guidelines, patients with OSCC who received primary treatment were scheduled to undergo imaging follow-up—including ^{18}F-FDG PET/CT, CT, or MRI scans—every three months for the first year and every six months thereafter. Enrollment encompassed a 17-year period (2004–2021) during which different editions of the American Joint Committee on Cancer (AJCC) Staging Manual were applied; for consistency, all patients included in the study were staged according to the eighth edition of the AJCC Staging Manual [19]. Patient characteristics—including risky oral habits (i.e., lifetime smoking and alcohol use) and the date of suspected mandibular involvement—were retrospectively extracted from clinical records.

Outcome definition

Mandibular relapse-free survival (MRFS)—defined as the time elapsed from the termination of primary RT to the date of mandibular cancer recurrence confirmed by histopathology—served as the main outcome measure. Censoring was performed on the date of the last follow-up (i.e., administrative censoring) for those without mandibular cancer recurrence.

^{18}F-FDG PET/CT acquisition

The median time interval between PET imaging and the results of histopathology was 41 days (interquartile range: 14–93 days). Patients underwent PET/CT imaging procedures on either a Discovery ST 16 scanner (GE Healthcare, Milwaukee, WI, USA) or a Biograph mCT scanner (Siemens Medical Solutions, Malvern, PA, USA) after a 6-h fast. The injected ^{18}F-FDG dose ranged between 370 and 555 MBq according to the patient's body weight. No intravenous contrast agent was used for CT scans.

Images were reconstructed using an ordered-subset expectation maximization (OSEM) algorithm (4 iterations and 10 subsets for the Discovery ST16 scanner; 2 iterations and 21 subsets for the Biograph mCT scanner, respectively). The values of axial spatial resolution at the center of the gantry were 4.80 (Discovery ST16 scanner) and 2.16 mm (Biograph mCT scanner), respectively.

^{18}F-FDG PET image analysis

In accordance with previous studies in the field of head and neck malignancies [16, 20], a fixed SUVmax threshold of 40% (T40) was used for segmentation of mandibular lesions. A SUVmax threshold of 99.9% was applied to localize the SUVmax voxel; upon identification of this voxel of interest (VOI), we measured the mean Hounsfield Unit (HU) on the corresponding CT images. The SUVmax VOI was considered located with bone predominance when the mean CT HU was > 275 [21] in all other cases, a soft tissue predominance localization was assigned. Segmentation of mandibular lesions and SUVmax localization were accomplished by two experienced nuclear medicine physicians (N.-M.C. and T.-C.Y.) who were blinded to clinical and pathological data. All decisions were taken by consensus.

Radiomics

PET radiomics features were extracted from VOI using the intensity histogram, gray-level co-occurrence matrix (GLCM), gray-level run-length matrix (GLRLM), and gray-level size zone matrix (GLSZM). A relative resampling method (64 bins) was applied to minimize noise that resulted from image processing [22]. PET radiomics parameters were calculated using the Chang-Gung Image Texture Analysis toolbox (CGITA) [23]. The terms and equations of PET texture parameters and the calculation procedures were consistent with the tenets set forth by the Imaging Biomarker Standardization Initiative (IBSI) [24].

Statistical analysis

The associations between the study variables were determined by calculating Spearman's correlation coefficients (ρ). Receiver operating characteristic (ROC) curve analysis was performed to select clinical variables and PET parameters associated with MRFS. All variables that produced an area under the ROC curve significantly different from 0.5 were included in subsequent analyses. The Youden's statistic was used to determine the optimal cut-off points for variables associated with MRFS. Patients were dichotomized based on the identified cut-off values for subsequent survival analyses. MRFS curves were plotted using the Kaplan–Meier method and compared with log-rank tests. Independent predictors of MRFS were identified using univariate and multivariate Cox proportional hazards regression models. Schoenfeld residuals were applied to assess the proportional hazards assumption. To minimize overfitting during model construction, we relied on the general rule of thumb for multivariate analysis [25]. Results are expressed as hazard ratios (HRs) with 95% confidence intervals (CIs). On analyzing the predictive ability of different parameters, we compared the concordance index (*C*-index) of each variable using a nonparametric approach implemented in MedCalc, version 19.1 (Mariakerke, Belgium) [26]. All other data were analyzed using SPSS, version 16.0 (SPSS Inc., Chicago, IL, USA), with all tests two-sided at a 5% level of significance.

Results

General characteristics of the study patients

Table 1 shows the general characteristics of the 103 study participants. Most patients were men and had a positive history of risky oral habits—including tobacco smoking and alcohol drinking. The most common tumor site was buccal carcinoma followed by tongue carcinoma. Most patients presented with advanced T-stage disease, although nodal involvement was relatively limited. The majority of the study participants were treated with radical surgery followed by post-operative concurrent chemoradiotherapy (CCRT) for their primary cancer. The median radiation dose in the entire study cohort was 66 Gy (range 60–88 Gy)—with the radiation field including the jaw in all cases. Ninety-four cases had received postoperative RT or CCRT in this study. Among them, ninety cases (95.7%) had RT dose within the range of 60–66 Gy. Four patients (4.3%) who had margin positive or extranodular extension had received additional boost RT (total dose: 68–88 Gy). Nevertheless, the RT dose did not associate with mandible cancer recurrence (area under the ROC curve: 0.536, $P = 0.620$) in our study. At the time of PET imaging, 41 patients (39.80%) had evidence of cancer recurrence or a second primary head and neck malignancy.

Mandibular cancer recurrence: associations with clinical and imaging parameters

Every patient underwent surgery for ORN or cancer recurrence in our study (12 patients underwent excisional biopsies; 65 cases underwent limited sequestrectomy and debridement; 10 patients received radical sequestrectomy and flap reconstruction; 16 ones underwent cancer-wide excision). The results of histopathology revealed that mandibular cancer recurrence occurred in 24 (23.30%) study participants (eight cases were proved by excisional biopsies; two patients by limited sequestrectomy and debridement; 14 ones by wide excision).

Table 1 General characteristics of the study patients ($n=103$) and univariate Cox regression analysis for mandibular relapse-free survival

Characteristic		*n* (%)	HR (95% CI)	*P*
Age at diagnosis	≤ 52 years	45 (43.69)	3.87 (1.59–9.42)	0.003
	> 52 years	58 (56.31)		
Sex	Female	5 (4.9)		
	Male	98 (95.1)	22.76 (0.02–34,393)	0.403
History of smoking	Yes	88 (85.44)	2.64 (0.61–11.37)	0.193
History of alcohol use	Yes	72 (69.90)	0.86 (0.38–1.97)	0.722
Diabetes	Yes	24 (23.30)	0.95 (0.35–2.55)	0.914
Cancer sites	Buccal	36 (34.95)	1.07 (0.46–2.46)	0.882
	Tongue	29 (28.16)		
	Gum	22 (21.36)		
	Mouth floor	8 (7.77)		
	Other sites*	8 (7.77)		
T stage	T1–T2	32 (31.07)		
	T3–T4	71 (68.93)	2.95 (0.87–9.98)	0.081
N stage	N-negative	51 (49.51)		
	N-positive	52 (50.49)	1.01 (0.45–2.27)	0.983
AJCC stage	I–II	16 (15.53)		
	III–IV	87 (84.47)	1.28 (0.38–4.35)	0.689
Primary treatment	Surgery plus CCRT	76 (73.79)	0.45 (0.19–1.06)	0.067
	Surgery plus RT	18 (17.48)		
	IC plus CCRT	7 (6.80)		
	CCRT	2 (1.94)		
SUV_{max} voxel site	Soft tissue predominance	60 (58.25)	5.08 (1.51–17.08)	0.009
	Bone predominance	43 (41.75)		
PET/CT parameters	SUVmax > 12.35	36 (34.95)	4.22 (1.74–10.23)	0.001
	SUVmax ≤ 12.35	67 (65.05)		
	TLG > 62.68	25 (24.27)	7.23 (3.08–16.98)	< 0.001
	TLG ≤ 62.68	78 (75.73)		

HR hazard ratio, *CI* confidence interval, *CCRT* concurrent chemoradiotherapy, *RT* radiotherapy, *IC* induction chemotherapy, *AJCC* American Joint Committee on Cancer, *SUVmax* maximum standardized uptake value, *TLG* total lesion glycolysis

*Other sites included hard palate ($n=2$), lip ($n=2$), soft palate ($n=2$), and tonsils ($n=2$)

Two patients underwent surgery of wide excision, but the pathological reports revealed only ORN.

The median follow-up time was 48.0 months (interquartile range: 31.5–67.4 months) in the entire cohort. For patients with ORN and mandibular recurrences, the follow-up time was 18.4 months and 26.5 months with corresponding interquartile ranges of 9.6–42.6 and 13.1–73.4 months, respectively. Recurrent subgroup tended to have longer follow-up time than ORN one with marginal significance ($P=0.109$). However, the follow-up time could not differentiate ORN from recurrence (area under the ROC curve: 0.616, $P=0.087$). On univariate Cox regression analysis (Table 1), an age at onset ≤ 52 years was associated with an increased risk of mandibular cancer recurrence ($P=0.003$). Associations of borderline statistical significance were observed for T3–T4 disease and treatment with radical surgery followed by post-operative CCRT. Mandibular cancer recurrence did not show significant associations with other clinical variables.

On analyzing PET parameters, a voxel site of SUVmax with soft tissue predominance, increased total lesion glycolysis (TLG), and elevated SUVmax values were all significantly associated with an increased likelihood of mandibular cancer recurrence (Table 1). ROC curve analyses of TLG, SUVmax, and other radiomics parameters are presented in Additional file 1: Table S1. Patients with mandibular cancer recurrence had higher TLG (104.34 ± 111.42 g vs. 38.86 ± 28.87 g, respectively, $P<0.001$) and SUVmax values (15.45 ± 7.62 vs. 9.80 ± 3.67, respectively, $P<0.001$) compared with those without. Upon calculation of the maximum Youden's indices, TLG and SUVmax values were dichotomized according to their optimal cut-off values (TLG > 62.68 vs. ≤ 62.68; SUVmax > 12.35 vs. ≤ 12.35).

A TLG > 62.68 g was not significantly correlated with either age ≤ 52 years ($\rho = 0.05$, $P = 0.622$) or a voxel site of SUVmax ($\rho = 0.07$, $P = 0.508$). However, significant correlations were observed for a SUVmax > 12.35 (age ≤ 52 years: $\rho = 0.216$, $P = 0.028$; voxel site of SUVmax with soft tissue predominance, $\rho = 0.249$, $P = 0.011$). A significant correlation was also noted between a TLG > 62.68 g and a SUVmax > 12.35 ($\rho = 0.297$, $P = 0.002$).

Predictors of mandibular recurrence-free survival

Kaplan–Meier plots of MRFS according to different clinical and PET parameters are reported in Fig. 1. Less favorable MRFS was observed for patients with an age at diagnosis ≤ 52 years, a voxel site of SUVmax with soft tissue predominance, and a TLG > 62.68 g. Because of the collinearity between SUVmax and TLG, these parameters were entered separately into multivariate analysis (Model 1 and Model 2, respectively; Table 2). The results revealed that a TLG > 62.68 g, an age at diagnosis ≤ 52 years, and a voxel site of SUVmax with soft tissue predominance were independent adverse prognostic factors for MRFS.

Prognostic scoring system for the prediction of mandibular recurrence-free survival

Finally, we devised a prognostic scoring system for the prediction of MRFS based on the three independent adverse prognostic factors identified from multivariate analysis (0 for the absence and 1 for the presence). The following distribution of risk scores was observed in the study cohort: score 0, $n = 18$; score 1, $n = 50$; score 2; $n = 25$; and score 3, $n = 10$. Mandibular cancer recurrence was observed in 0 (0%), 3 (6%), 12 (48%), and 9 (90%) patients with a score of 0, 1, 2, and 3, respectively. Patients with score of 2–3 were considered at high risk, whereas those with a score of 0 or 1 were a low-risk group. High-risk patients had a significantly higher likelihood of mandibular cancer recurrence (HR 32.50, 95% CI 8.51–124.18, $P < 0.001$).

The scoring system had a sensitivity of 87.50%, a specificity of 82.28%, and an overall accuracy of 83.50% for

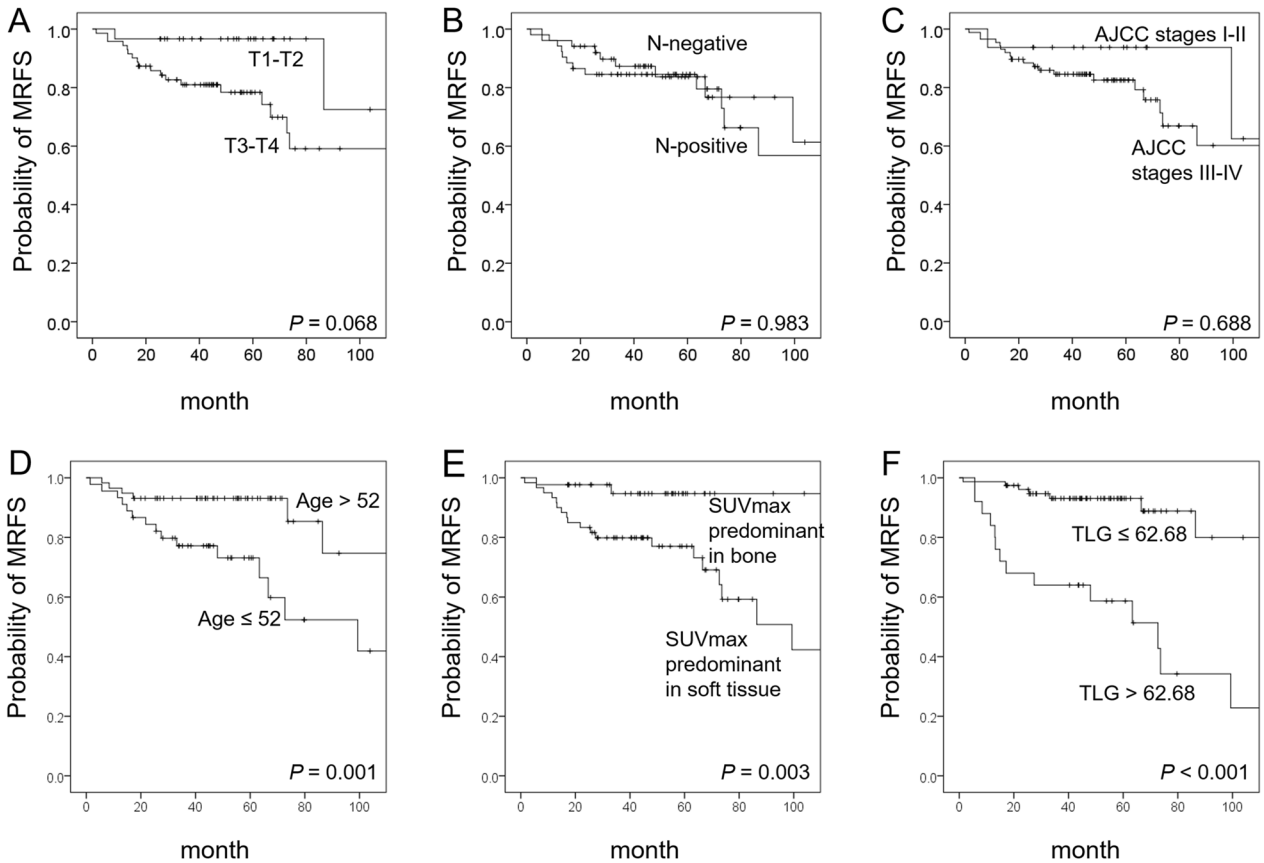

Fig. 1 Kaplan–Meier plots of mandibular relapse-free survival (MRFS) rates in patients with OSCC stratified according to T stage (**A**), N stage (**B**), AJCC stage (**C**), age at cancer diagnosis (**D**), SUVmax site (**E**), and TLG (**F**). The Youden's statistic was used to determine the optimal cut-off point for each variable. *P* values according to log-rank tests are presented in the insets

Table 2 Multivariable Cox regression analysis of mandibular relapse-free survival

Variable	HR (95% CI)	*P*
Model 1		
Age at diagnosis ≤ 52 years	3.36 (1.31–8.64)	0.012
Voxel site of SUVmax with soft tissue predominance	5.02 (1.45–17.31)	0.011
SUVmax > 12.35	2.38 (0.94–6.06)	0.068
Model 2		
Age at diagnosis ≤ 52 years	3.36 (1.30–8.73)	0.013
Voxel site of SUVmax with soft tissue predominance	4.35 (1.27–14.90)	0.019
TLG > 62.68 g	5.38 (2.24–12.91)	< 0.001

HR hazard ratio, *CI* confidence interval, *SUVmax* maximum standardized uptake value, *TLG* total lesion glycolysis

identifying mandibular cancer recurrence. As Fig. 2 shows, the scoring system (*C*-index = 0.85) outperformed several parameters—including T3–T4 disease (*C*-index = 0.59, $P < 0.001$), treatment with surgery and post-operative CCRT (*C*-index = 0.57, $P < 0.001$), age at diagnosis ≤ 52 years (*C*-index = 0.68, $P = 0.002$), a voxel site of SUVmax within soft tissue (*C*-index = 0.69, $P < 0.001$), and high TLG values (*C*-index = 0.73, $P = 0.052$)—for the prediction of MRFS. Figure 3 shows illustrative PET images obtained in high- versus low-risk patients.

Discussion

The clinical outcomes of patients with OSCC who had undergone primary multidisciplinary treatment remain heterogeneous [27]. Although recent years have witnessed significant technical advances in the field of RT techniques, mandibular ORN remains a significant clinical concern. Here, we demonstrate that a simple scoring system—based on the presence of a mandibular TLG > 62.68 g, an age at diagnosis ≤ 52 years, and a voxel site of SUVmax located with soft tissue predominance—was clinically useful for identifying patients at high risk of mandibular cancer recurrence. In addition, the scoring system provided a reliable stratification of MRFS in patients with OSCC.

This is, to our knowledge, the first study to provide a comprehensive analysis of clinical variables and PET imaging parameters in relation to the risk of mandibular cancer recurrence in patients with suspected ORN of the jaw. As far as PET variables are concerned, we found that TLG—a parameter which provides information regarding both lesion volume and metabolic activity—outperformed the predictive value of SUVmax for mandibular cancer recurrence. It is possible that the high collinearity of mandible SUVmax with age at diagnosis and the SUVmax voxel site could have attenuated its clinical significance in the prediction of mandibular cancer recurrence. Another interesting finding from our study is the predictive value of a voxel site of

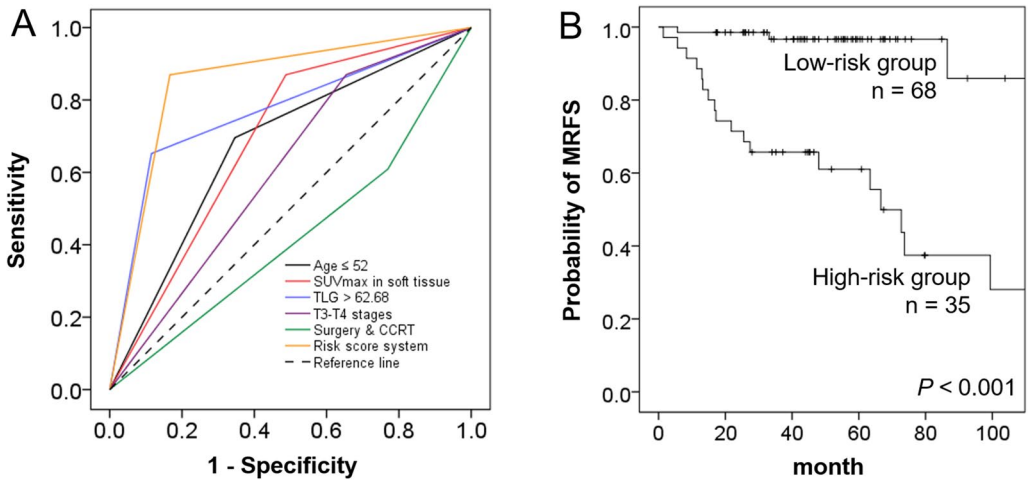

Fig. 2 Receiver operating characteristic curve analyses and *C*-indices for the prediction of MRFS (**A**). The *C*-index of the simple scoring system was higher than those calculated for other parameters. Kaplan–Meier plots of MRFS in patients with OSCC classified as being at low- versus high-risk according to the simple scoring system (**B**). *P* values according to log-rank tests are presented in the insets

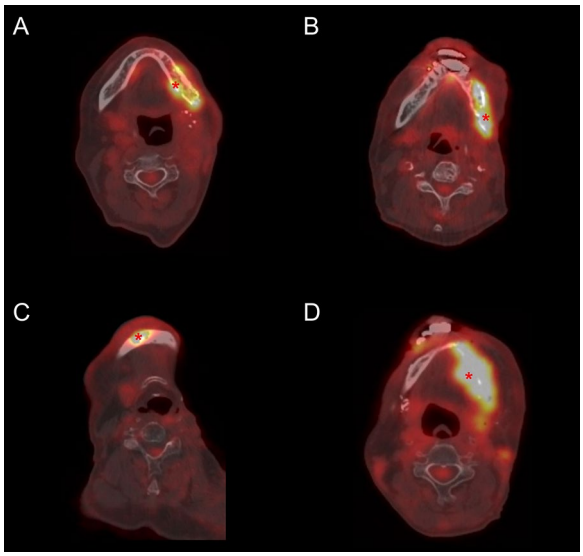

Fig. 3 PET/CT image **A** obtained from a patient with left buccal cancer (T3N2bM0; AJCC stage IVA) diagnosed at 59 years of age. The patient had an elevated mandibular TLG (149.28 g, see main text), but the voxel site of SUVmax (asterisk) was located with bone predominance (CT HU: 340.0). A score of 1 was assigned. The results of histopathology revealed the presence of mandibular osteoradionecrosis (ORN). PET/CT image **B** obtained from a patient with left buccal cancer (T3N1M0; AJCC stage III) diagnosed at 56 years of age. The patient had an elevated mandibular TLG (73.66 g) and showed a voxel site of SUVmax located with soft tissue predominance (asterisk) (CT HU: 186.0). A score of 2 was assigned. The results of histopathology revealed the presence of mandibular cancer recurrence. PET/CT image **C** obtained from a patient with left buccal cancer (T3N2bM0; AJCC stage IVA) diagnosed at 67 years of age. The patient had a low mandibular TLG (51.27 g) and showed a voxel site of SUVmax located with soft tissue predominance (asterisk) (CT HU: 97.2). A score of 1 was assigned. The results of histopathology revealed the presence of mandibular ORN. PET/CT image **D** obtained from a patient with a score of 3. He was diagnosed with left lower gum cancer (T2N0M0, stage II) at 45 years of age. The patient had an elevated mandibular TLG (175.47 g) and showed a voxel site of SUVmax located with soft tissue predominance (asterisk) (CT HU: 18.0). The results of histopathology revealed the presence of mandibular cancer recurrence

SUVmax located with soft tissue predominance, which is in accordance with the study by Meerwein et al. [11]. It is well-known that cancer recurrences tend to occur in soft tissues characterized by abundant vascular networks rather than in poorly vascularized bone structures. However, malignant cells located in close proximity to osseous tissue may activate osteoclastogenesis and ultimately promote both bone resorption and cancer dissemination [28, 29]. Although this may offer an explanation for the observed association between a voxel site of SUVmax located within soft tissue and mandibular cancer recurrence, further mechanistic studies are warranted.

Differently from TLG and SUVmax, PET radiomics parameters did not show significant associations with MRFS in our study. While the exact underlying reasons remain unclear, it is possible that the use of two different CT attenuation maps (i.e., bone and soft tissue) during PET image reconstruction of mandibular lesions might have played a role. Accordingly, there is evidence that an elevated noise and image misregistration may lead to inaccurate estimation of radiomics parameters [24, 30, 31].

The impact of patient age on the clinical outcomes of OSCC is a matter of ongoing debate [32]. In our study, an age at diagnosis ≤ 52 years was identified as an adverse prognostic factor for MRFS. It has been previously reported that young patients with OSCC tend to show a higher immunohistochemical expression of p53 in malignant tissues [33]—which in turn represents an unfavorable prognostic biomarker [34–37]. Our findings may prompt additional investigations on the association between p53 expression and the occurrence of mandibular cancer recurrence in OSCC.

The scoring system devised in our study may have major clinical implications for the differential diagnosis of mandibular lesions in patients with OSCC who had undergone primary RT. In general, the following strategy can be applied for patients with suspected ORN of the jaw following RT. Since mandibular cancer recurrence occurred very rarely in low-risk patients (4.41%), biopsy can be avoided and traditional surgical management for ORN of the jaw should be sufficient. However, high-risk patients require second-level diagnostic procedures—including histopathological analysis of biopsy samples—for ruling out the presence of mandibular cancer recurrence. Further research is necessary to examine the clinical appropriateness of the proposed scoring system.

There are limitations to this study. First, this is a single-center investigation and the results clearly require replication. The retrospective nature of this study is prone to unavoidable confounding and residual confounding and a selection bias cannot be excluded. Second, our research was specifically focused on PET parameters and the potential diagnostic value of CT imaging patterns was not taken into account. However, the significance of an infiltrative growth pattern on CT images is not univocal and may reflect either the presence ORN [12] or tumor recurrence [11]. Finally, we acknowledge that lesion segmentation and the localization of SUVmax site were based partly on visual interpretation—which is prone to inter-observer variability.

Conclusion

The scoring system described in our study may be clinically useful for identifying mandibular cancer recurrence in patients with OSCC and suspected ORN of the jaw. High-risk patients may benefit from a diagnostic biopsy for ruling out the presence of tumor recurrence, whereas the use of histopathology can be avoided in those with a score of 0 or 1. Our findings should be considered as hypothesis-generating and require validation in independent clinical cohorts.

Supplementary Information

The online version contains supplementary material available at https://doi.org/10.1186/s13550-023-00965-8.

Additional file 1. Supplementary Table 1.

Acknowledgements
Not applicable.

Author contributions
NMC, CYL, TCY conceived and designed the experiments. NMC, CYL, CTL, TCY performed the experiments. All authors analyzed the data. NMC, CYL, CTL, DLT, SHN, and TCY contributed reagents/materials/analysis tools. NMC, CYL, TCY wrote the paper. All authors read and approved the final manuscript.

Funding
This study was financially supported by a Grant (MOST 111-2314-B-182A-046) from the Ministry of Science and Technology, Taiwan.

Availability of data and materials
The datasets used and/or analyzed during the current study are available from the corresponding author on reasonable request.

Declarations

Ethics approval and consent to participate
The study protocol was approved by the Institutional Review Board of Chang Gung Medical Foundation (approval numbers: 202102071B0). The requirement for written patient informed consent was waived due to the retrospective study design. All study procedures were in accordance with the ethical standards of the institutional and national research committee and with the principles of the 1964 Declaration of Helsinki and its later amendments.

Consent for publication
Not applicable.

Competing interests
The authors declare no competing interests.

Received: 19 December 2022 Accepted: 7 February 2023
Published online: 03 April 2023

References

1. Reuther T, Schuster T, Mende U, Kübler A. Osteoradionecrosis of the jaws as a side effect of radiotherapy of head and neck tumour patients—a report of a thirty year retrospective review. Int J Oral Maxillofac Surg. 2003;32:289–95. https://doi.org/10.1054/ijom.2002.0332.
2. Pitak-Arnnop P, Sader R, Dhanuthai K, Masaratana P, Bertolus C, Chaine A, et al. Management of osteoradionecrosis of the jaws: an analysis of evidence. Eur J Surg Oncol J Eur Soc Surg Oncol Br Assoc Surg Oncol. 2008;34:1123–34. https://doi.org/10.1016/j.ejso.2008.03.014.
3. Möring MM, Mast H, Wolvius EB, Verduijn GM, Petit SF, Sijtsema ND, et al. Osteoradionecrosis after postoperative radiotherapy for oral cavity cancer: a retrospective cohort study. Oral Oncol. 2022;133:106056. https://doi.org/10.1016/j.oraloncology.2022.106056.
4. Chang CT, Liu SP, Muo CH, Liao YF, Chiu KM, Tsai CH, et al. The impact of dental therapy timelines and irradiation dosages on osteoradionecrosis in oral cancer patients: a population-based cohort study. Oral Oncol. 2022;128:105827. https://doi.org/10.1016/j.oraloncology.2022.105827.
5. Marx RE. A new concept in the treatment of osteoradionecrosis. J Oral Maxillofac Surg Off J Am Assoc Oral Maxillofac Surg. 1983;41:351–7. https://doi.org/10.1016/s0278-2391(83)80005-6.
6. Jacobson AS, Buchbinder D, Hu K, Urken ML. Paradigm shifts in the management of osteoradionecrosis of the mandible. Oral Oncol. 2010;46:795–801. https://doi.org/10.1016/j.oraloncology.2010.08.007.
7. Wang CC, Cheng MH, Hao SP, Wu CC, Huang SS. Osteoradionecrosis with combined mandibulotomy and marginal mandibulectomy. Laryngoscope. 2005;115:1963–7. https://doi.org/10.1097/01.mlg.0000178374.29219.5e.
8. Davis DD, Hanley ME, Cooper JS. Osteoradionecrosis. Treasure Island: StatPearls; 2022.
9. Zehr LJ, Cooper JS. Mandible osteoradionecrosis. Treasure Island: StatPearls Publishing; 2022.
10. Sanli Y, Zukotynski K, Mittra E, Chen DL, Nadel H, Niederkohr RD, et al. Update 2018: 18F-FDG PET/CT and PET/MRI in head and neck cancer. Clin Nucl Med. 2018;43:e439–52. https://doi.org/10.1097/rlu.0000000000002247.
11. Meerwein CM, Nakadate M, Stolzmann P, Vital D, Morand GB, Zweifel DF, et al. Contrast-enhanced 18F-FDG-PET/CT for differentiating tumour and radionecrosis in head and neck cancer: our experience in 37 patients. Clin Otolaryngol Off J ENT-UK Off J Neth Soc Oto-Rhino-Laryngol Cervico-Fac Surg. 2018;43:1594–9. https://doi.org/10.1111/coa.13185.
12. Alhilali L, Reynolds AR, Fakhran S. Osteoradionecrosis after radiation therapy for head and neck cancer: differentiation from recurrent disease with CT and PET/CT imaging. AJNR Am J Neuroradiol. 2014;35:1405–11. https://doi.org/10.3174/ajnr.A3879.
13. Sonoda LI, Lakhani A, Ghosh-Ray S. Prevalence of osteoradionecrosis demonstrated in 18F-FDG PET-CT of post-high-dose-radiotherapy head and neck cancer patients. Cancer Imaging. 2014;14:P3. https://doi.org/10.1186/1470-7330-14-s1-p3.
14. Hung GU, Tsai SC, Lin WY. Extraordinarily high F-18 FDG uptake caused by radiation necrosis in a patient with nasopharyngeal carcinoma. Clin Nucl Med. 2005;30:558–9. https://doi.org/10.1097/01.rlu.0000170039.14351.0b.
15. Yamada S, Kubota K, Kubota R, Ido T, Tamahashi N. High accumulation of fluorine-18-fluorodeoxyglucose in turpentine-induced inflammatory tissue. J Nucl Med Off Publ Soc Nucl Med. 1995;36:1301–6.
16. Cheng NM, Hsieh CE, Fang YD, Liao CT, Ng SH, Wang HM, et al. Development and validation of a prognostic model incorporating [(18)F]FDG PET/CT radiomics for patients with minor salivary gland carcinoma. EJNMMI Res. 2020;10:74. https://doi.org/10.1186/s13550-020-00631-3.
17. Creff G, Devillers A, Depeursinge A, Palard-Novello X, Acosta O, Jegoux F, et al. Evaluation of the prognostic value of FDG PET/CT parameters for patients with surgically treated head and neck cancer: a systematic review. JAMA Otolaryngol Head Neck Surg. 2020;146:471–9. https://doi.org/10.1001/jamaoto.2020.0014.
18. Cheng NM, Kang CJ, Tsai CY, Lee LY, Lin CY, Hsueh C, et al. Improved prognostic stratification of patients with pN3b oral cavity cancer based on maximum standardized uptake value of metastatic nodes, lymph node ratio, and level of cervical nodal metastases. Oral Oncol. 2021;123:105593. https://doi.org/10.1016/j.oraloncology.2021.105593.
19. Amin MB, Edge SB, Greene FL, Byrd DR, Brookland RK, Washington MK, et al. AJCC cancer staging manual. 8th ed. New York: Springer; 2017.
20. Rasmussen JH, Nørgaard M, Hansen AE, Vogelius IR, Aznar MC, Johannesen HH, et al. Feasibility of multiparametric imaging with PET/MR in head and neck squamous cell carcinoma. J Nucl Med Off Publ Soc Nucl Med. 2017;58:69–74. https://doi.org/10.2967/jnumed.116.180091.
21. Hiasa K, Abe Y, Okazaki Y, Nogami K, Mizumachi W, Akagawa Y. Preoperative computed tomography-derived bone densities in hounsfield units at implant sites acquired primary stability. ISRN Dent. 2011;2011:678729. https://doi.org/10.5402/2011/678729.

22. Desseroit MC, Tixier F, Weber WA, Siegel BA, Cheze Le Rest C, Visvikis D, et al. Reliability of PET/CT shape and heterogeneity features in functional and morphologic components of non-small cell lung cancer tumors: a repeatability analysis in a prospective multicenter cohort. J Nucl Med Off Publ Soc Nucl Med. 2017;58:406–11. https://doi.org/10.2967/jnumed.116.180919.
23. Fang YH, Lin CY, Shih MJ, Wang HM, Ho TY, Liao CT, et al. Development and evaluation of an open-source software package "CGITA" for quantifying tumor heterogeneity with molecular images. BioMed Res Int. 2014;2014:248505. https://doi.org/10.1155/2014/248505.
24. Zwanenburg A, Vallières M, Abdalah MA, Aerts H, Andrearczyk V, Apte A, et al. The image biomarker standardization initiative: standardized quantitative radiomics for high-throughput image-based phenotyping. Radiology. 2020;295:328–38. https://doi.org/10.1148/radiol.2020191145.
25. Riley RD, Snell KI, Ensor J, Burke DL, Harrell FE Jr, Moons KG, et al. Minimum sample size for developing a multivariable prediction model: PART II—binary and time-to-event outcomes. Stat Med. 2019;38:1276–96. https://doi.org/10.1002/sim.7992.
26. DeLong ER, DeLong DM, Clarke-Pearson DL. Comparing the areas under two or more correlated receiver operating characteristic curves: a nonparametric approach. Biometrics. 1988;44:837–45.
27. Tseng YJ, Wang HY, Lin TW, Lu JJ, Hsieh CH, Liao CT. Development of a machine learning model for survival risk stratification of patients with advanced oral cancer. JAMA Netw Open. 2020;3:e2011768. https://doi.org/10.1001/jamanetworkopen.2020.11768.
28. Jimi E, Furuta H, Matsuo K, Tominaga K, Takahashi T, Nakanishi O. The cellular and molecular mechanisms of bone invasion by oral squamous cell carcinoma. Oral Dis. 2011;17:462–8. https://doi.org/10.1111/j.1601-0825.2010.01781.x.
29. Koyama LKS, Nagano CP, Vanini JV, Figueredo JM Jr, Matos LL, Cernea CR, et al. Oral squamous cell carcinoma bone invasion: possible roles of E-cadherin in osteoclastogenesis and bone infiltration. ORL J Oto-Rhino-Laryngol Relat Spec. 2021;83:354–61. https://doi.org/10.1159/000514229.
30. Galavis PE, Hollensen C, Jallow N, Paliwal B, Jeraj R. Variability of textural features in FDG PET images due to different acquisition modes and reconstruction parameters. Acta Oncol (Stockholm, Sweden). 2010;49:1012–6. https://doi.org/10.3109/0284186x.2010.498437.
31. Yan J, Chu-Shern JL, Loi HY, Khor LK, Sinha AK, Quek ST, et al. Impact of image reconstruction settings on texture features in 18F-FDG PET. J Nucl Med Off Publ Soc Nucl Med. 2015;56:1667–73. https://doi.org/10.2967/jnumed.115.156927.
32. Chang TS, Chang CM, Ho HC, Su YC, Chen LF, Chou P, et al. Impact of young age on the prognosis for oral cancer: a population-based study in Taiwan. PLoS ONE. 2013;8:e75855. https://doi.org/10.1371/journal.pone.0075855.
33. De Paula AM, Souza LR, Farias LC, Corrêa GT, Fraga CA, Eleutério NB, et al. Analysis of 724 cases of primary head and neck squamous cell carcinoma (HNSCC) with a focus on young patients and p53 immunolocalization. Oral Oncol. 2009;45:777–82. https://doi.org/10.1016/j.oraloncology.2008.11.015.
34. Poeta ML, Manola J, Goldwasser MA, Forastiere A, Benoit N, Califano JA, et al. TP53 mutations and survival in squamous-cell carcinoma of the head and neck. N Engl J Med. 2007;357:2552–61. https://doi.org/10.1056/NEJMoa073770.
35. Monteiro LS, Diniz-Freitas M, Garcia-Caballero T, Warnakulasuriya S, Forteza J, Fraga M. Combined cytoplasmic and membranous EGFR and p53 overexpression is a poor prognostic marker in early stage oral squamous cell carcinoma. J Oral Pathol Med Off Publ Int Assoc Oral Pathol Am Acad Oral Pathol. 2012;41:559–67. https://doi.org/10.1111/j.1600-0714.2012.01142.x.
36. Gupta S, Khan H, Kushwaha VS, Husain N, Negi M, Ghatak A, et al. Impact of EGFR and p53 expressions on survival and quality of life in locally advanced oral squamous cell carcinoma patients treated with chemoradiation. Cancer Biol Ther. 2015;16:1269–80. https://doi.org/10.1080/15384047.2015.1070985.
37. Khan H, Gupta S, Husain N, Misra S, Mps N, Jamal N, et al. Correlation between expressions of Cyclin-D1, EGFR and p53 with chemoradiation response in patients of locally advanced oral squamous cell carcinoma. BBA Clin. 2015;3:11–7. https://doi.org/10.1016/j.bbacli.2014.11.004.

Publisher's Note

Springer Nature remains neutral with regard to jurisdictional claims in published maps and institutional affiliations.

Submit your manuscript to a SpringerOpen journal and benefit from:

- ► Convenient online submission
- ► Rigorous peer review
- ► Open access: articles freely available online
- ► High visibility within the field
- ► Retaining the copyright to your article

Submit your next manuscript at ► springeropen.com